Power Production and Economical Feasibility of Tideng Tidal Stream Power Converter

Parmeggiani, Stefano; Frigaard, Peter; Kofoed, Jens Peter; Rasmussen, Michael R.

Publication date:
2010

Document Version
Publisher's PDF, also known as Version of record

Power Production and Economical Feasibility of Tideng Tidal Stream Power Converter

S. Parmeggiani
P. Frigaard
J. P. Kofoed
M. Rasmussen

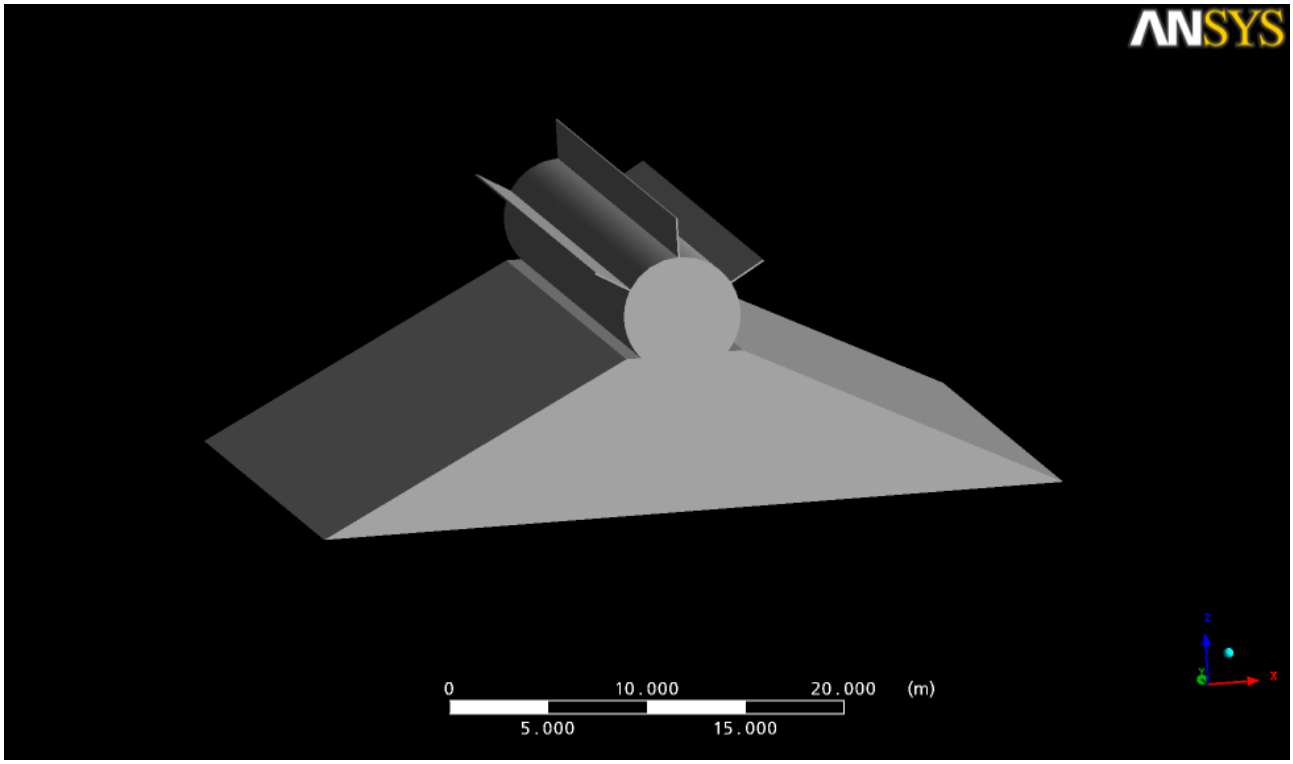

ISSN 1901-726X
DCE Technical Report No. 81

AALBORG UNIVERSITY
Department of Civil Engineering

Aalborg University
Department of Civil Engineering
Water and Soil
Wave Energy Research Group

DCE Technical Report No. 81

Power production and economical feasibility of Tideng tidal stream power converter

by

S. Parmeggiani
P. Frigaard
J. P. Kofoed
M. Rasmussen

May 2010

Scientific Publications at the Department of Civil Engineering

Technical Reports are published for timely dissemination of research results and scientific work carried out at the Department of Civil Engineering (DCE) at Aalborg University. This medium allows publication of more detailed explanations and results than typically allowed in scientific journals.

Technical Memoranda are produced to enable the preliminary dissemination of scientific work by the personnel of the DCE where such release is deemed to be appropriate. Documents of this kind may be incomplete or temporary versions of papers—or part of continuing work. This should be kept in mind when references are given to publications of this kind.

Contract Reports are produced to report scientific work carried out under contract. Publications of this kind contain confidential matter and are reserved for the sponsors and the DCE. Therefore, Contract Reports are generally not available for public circulation.

Lecture Notes contain material produced by the lecturers at the DCE for educational purposes. This may be scientific notes, lecture books, example problems or manuals for laboratory work, or computer programs developed at the DCE.

Theses are monograms or collections of papers published to report the scientific work carried out at the DCE to obtain a degree as either PhD or Doctor of Technology. The thesis is publicly available after the defence of the degree.

Latest News is published to enable rapid communication of information about scientific work carried out at the DCE. This includes the status of research projects, developments in the laboratories, information about collaborative work and recent research results.

Published 2010 by
Aalborg University
Department of Civil Engineering
Sohngaardsholmsvej 57,
DK-9000 Aalborg, Denmark

Printed in Aalborg at Aalborg University

ISSN 1901-726X
DCE Technical Report No. 81

Recent publications in the DCE Technical Report Series

Kofoed, J. P. & Antonishen, M.: *The Crest Wing Wave Energy Device - 2nd phase testing*. DCE Technical Report No. 59. ISSN1901-726X. Dep. of Civil Eng., Aalborg University, Mar. 2009.

Kofoed, J. P. & Frigaard, P.: *Hydraulic evaluation of the LEANCON wave energy converter.* DCE Technical Report No. 45. ISSN1901-726X. Dep. of Civil Eng., Aalborg University, Oct. 2008.

Kofoed, J. P. & Frigaard, P. and Beserra, E. R.: *Wave induced loads on the LEANCON wave energy converter.* DCE Technical Report No. 44. ISSN1901-726X. Dep. of Civil Eng., Aalborg University, Oct. 2008.

Preface

This report is a product of the contract between Aalborg University and TIDENG (by Bent Hilleke) on the evaluation and development of the TIDENG Tidal Energy Conversion System (TECS). The work has focused on the evaluation of the yearly power production of the device and its economical feasibility, based on CFD simulations of the device under flow conditions typical of a possible location for the deployment at the Faeroer Island.

The report has been prepared by PhD student Stefano Parmeggiani in co-operation with associate professor Peter Frigaard, associate professor Jens Peter Kofoed and associate professor Michael Rasmussen, all from the Wave Energy Research Group at Department of Civil Engineering, Aalborg University.

Stefano Parmeggiani
Sohngaardsholmsvej 57, Room: C-211
DK-9000 Aalborg, Denmark
sp@civil.aau.dk

Peter Frigaard
Sohngaardsholmsvej 57, Room: C-221
DK - 9000 Aalborg
pf@civil.aau.dk
Phone: 9940 8479

Jens Peter Kofoed
Sohngaardsholmsvej 57, Room: C-226
DK - 9000 Aalborg
jpk@civil.aau.dk
Phone: 9940 8474

Michael Rasmussen
Sohngaardsholmsvej 57, Room: C-204
DK - 9000 Aalborg
mr@civil.aau.dk
Phone: 9940 8485

Aalborg, March 2010

Table of contents

1. INTRODUCTION

Tidal energy

Tide is the deformation of the surface of the Earth, particularly evident in the oceans, generated by its gravitational interaction with other celestial bodies, mainly the Moon.
Based on periodical phenomena such as the celestial motions, tide is in principle highly predictable, and the extraction of tidal energy has a huge potential all around the world.

Tidal energy can be harnessed both in the potential or kinetic form. In the first case the difference in the water level between high tide and low tide is used to drive turbines in structures like dams, called *tidal barrages*. In *tidal stream systems* instead, as is the case of Tideng, turbines are submerged to exploit the kinetic energy of tidal currents, with a working principle similar to that of windmills. These can be deployed in arrays, and are usually characterized by lower environmental impact and construction costs than tidal barrages.

The magnitude of the energy extracted is proportional to the difference in height (head) between low and high tide for tidal barrages, and to the cube of the flow velocity for tidal stream systems.

In both cases the choice of the deployment location is fundamental, as many physical characteristics such as bathimetry and morphology can have a big effect on the actual availability and magnitude of the resource. This makes tidal energy systems extremely site specific.
Generally speaking, better conditions will be found in zones such as estuaries, straights or wherever the local morphology causes the water section to suddenly narrow down. In these regions either the head will be bigger or the speed of tidal currents will be higher.

The Tideng TECS

Tideng is a tidal stream energy converter, a device which harnesses the energy of tidal currents to produce electricity.

It is composed by a cross-flow turbine with horizontal axis, supported by a base structure placed on the bottom of the sea. The base, besides providing the necessary stability to the device, enhances the incoming flow speed towards the rotor, which converts the kinetic energy of the flow into electricity as it is coupled to a generator.
The capture area is represented by the shadow area created by the device, equal to a vertical section of the device passing through the centre of rotation. As this is rectangular the space is used in an optimal way, making the device a modular unit which can be deployed in arrays or individually.

The rotor is the innovative and novel aspect of the device. The blades are connected at both ends to the fixed part of the hub by a joint which is moving along a path grooved in it. This path is designed so that, during the rotation, the blades are forced to move alternatively in and out of the rotor.

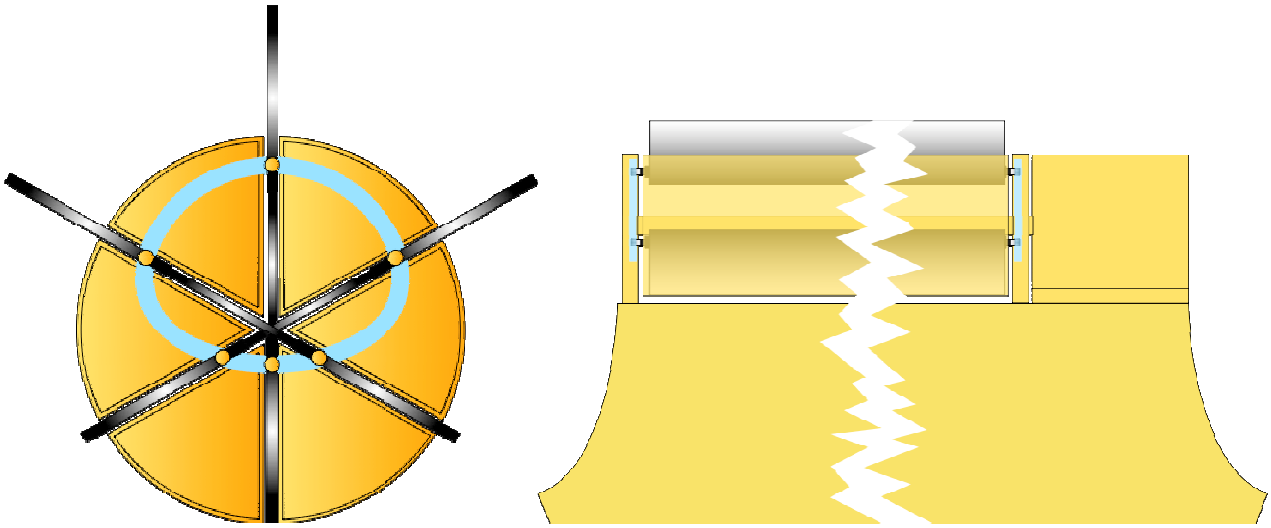

Figure 1.1 – The rotor and the device

Considering the section showed in Fig. 1.1, we can describe the blades' movement by assuming an orthogonal reference system with its origin at the centre of the rotor, the z-axis pointing upwards and the x-axis to the right (assumed as the flow direction). The blades, pushed by the flow, are rotating clockwise. If α is the angle they form with the horizontal axis, assuming it to be zero on the side of negative x, the extension of the active blades can be described as a function of α:

α	315°-45°	45°-135°	135°-225°	225°- 315°	0°; 180°
Extension	Increasing	Full	Decreasing	Null	Half

Table 1.1 – Blade's extension during the rotation

The described system balances the fact that, contrary to other kinds of turbine, the active blades do not take advantage of the lift effect. In fact this mechanism allows increasing the contact surface between the rotor and the flow in the region where this is more energetic, so to maximize the forces acting on the blades which determine the rotation. On the other hand, it decreases the resistance of the rotor to the movement in less energetic regions, where the blades would be pushing the water instead of being pushed. Moreover, this system limits the space needed for the blades' motion in between the rotor and the structure, avoiding parasite currents which would oppose to the rotation.
For all of these reasons, this patented system improves the hydraulic performances of the turbine and the overall efficiency of the device.

Previous studies

1. *Establishment of the model for the evaluation of the power production*

In January 2004, DHI (Institute for Water and Environment) provided the first model for evaluating the power production and the efficiency of the device [1].
The model considers a *current gain factor* to describe the effect of the structure in enhancing the velocity of the incoming flow U_{IN} towards the rotor. This is proportional to the flow section obstructed by the structure: $\boldsymbol{Cg = 1.3 \cdot d/(d-h)}$, where d is the water depth and h the height of the device. At the rotor the flow speed will be $U' = U_{IN} \cdot Cg$.

The power production is given by the product of the rotational speed of the rotor, ω [rad/s], times the total torque M [N · m] exerted on all the blades by the flow:

$$PP = \omega \cdot M \quad [W]$$

M is the torque of the pressure forces, which can be estimated through the Morrison's formula:

$$F = \tfrac{1}{2} \cdot \rho \cdot Cd \cdot A \cdot Urel^2 \quad [N]$$

where Cd is a drag coefficient, assumed 1.6, A is the blade's surface and $Urel$ is the relative velocity of the flow respect to the blade's one. $M = F \cdot b$, where b is the distance from the centre of rotation to the point of application of the force, which is assumed to be the centre of the blade.

Considering a steady state, the speed of the blades is equal to the speed of the surrounding flow; therefore the rotational speed of the turbine is $\omega = U'/r$, where r is the distance between the tip of the blades and the centre of the rotation.
The optimal power production, *PPopt*, is suggested to be achieved when the rotational speed is the 30% of ω, as if the rotor moves with the same velocity of the surrounding flow no force could be exterted on the blades ($Urel=0$) and no power would be produced.

Therefore the model estimates the best performance of the device as

$$\boldsymbol{PPopt = 0.3 \cdot \omega \cdot M} \quad \textbf{[W]}$$

By considering a uniform incoming flow of 4 m/s, a device 12 m high in 30 m water depth, with a 6 m diameter rotor and blades of 2 x 20 m, is estimated to produce **2.4 MW.** The same device, considering a harmonic tidal cycle with maximum velocity of 4 m/s, would have a yearly power production of 8.47 GWh.

2. *1:20 model test*

In 2007 some physical test on a 1:20 scale model of the device were conducted by Sintef Fisheries and Aquaculture in order to estimate the power production of the turbine [2]. The same power evaluation model was considered, $PP = \omega \cdot M$, and the *Froude scale theory* was used to upscale the results.
The rotational speed was evaluated by direct observation, measuring the RPM of one blade, while the torque was controlled by applying some load to the end of the rotor shaft through a brake disk.

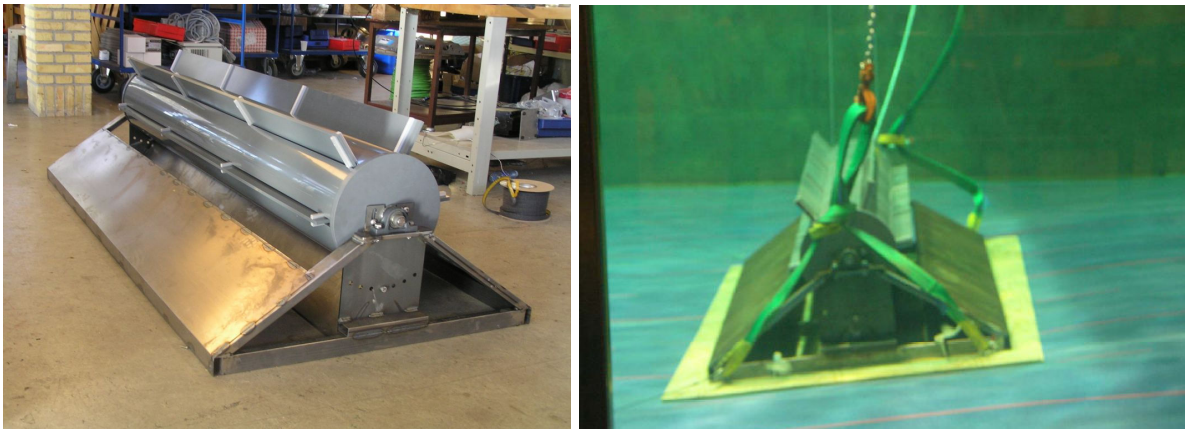

Figure 1.2 – The 1:20 scale prototype tested in 2007

16 different tests were conducted under different load conditions, so to establish a relationship between the torque applied on rotor by the brake and the consequent rotational speed.
The results showed that the optimal power production for a full scale device 7 m high in 54 m water depth, with a rotor diameter of 6 m and 2 x 38 m blades, was **0.98 MW** under a flow condition of 4 m/s. This was achieved at around the half of the maximum rotational speed, at a value of 0.44 rad/s.
Another remarkable result of the tests was that the dependence of the delivered power on small changes in the direction of the flow respect to the turbine is negligible.

3. *Numerical simulations*

In 2009 some numerical simulations have been performed by the authors at Aalborg University, Department of Civil Engineering, in order to improve the design of the base structure so to maximize its enhancing effect on the flow velocity, and to estimate the power production of the optimized geometry [3].
The simulations were carried out through Computational Fluid Dynamics (CFD), a computer based tool which solves iteratively the equations of fluid dynamics over a volume discretized by a net, called *mesh*, given intial and boundary conditions. The result provides the distribution of pressure on the wall boundaries and the velocity field through the domain at each node of the mesh.

Different parameters were considered in the optimization process, from geometrical variables to the position of the device and its orientation in the three dimensions.

(a) Stability

First of all the stability of the structure was assessed, neglecting the rotor as its influence is minor. For a trapezoidal structure 8 m high, with a 36 m base and a 1:2 steep profile, made of 10 cm thick concrete and under a 3 m/s flow, **the distribution of the pressure on the profile and the weight of the device determine more friction than the tangential forces can overcome.**
The friction force opposing to the movement is given by the sum of the weight plus the vertical component of the pressure force acting on the profile times a friction coefficient, which for concrete on rock can be assumed 0.35. This was $1.68 \cdot 10^6$ N, more that 5 times bigger than the unbalancing tangential component of the pressure force acting on the structure, which was found to be $3 \cdot 10^5$ N.
As a result the structure is stable, since in such configuration the flow pushes the structure against the bottom, ensuring no slip or rotation.

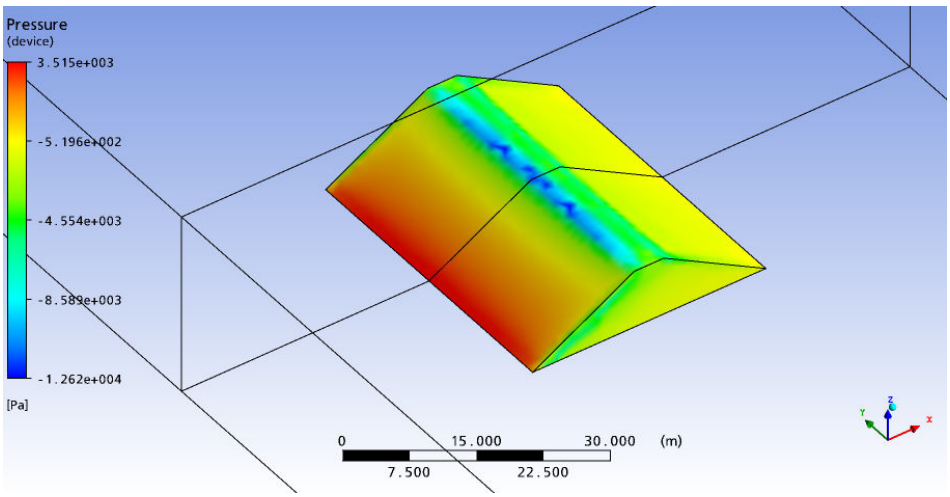

Figure 1.3 – Pressure distribution on the base structure

(b) Geometry optimization

A 2-D configuration has been considered in this phase, in order to determine the influence of different parameters on the current gain factor. As the focus was on the base structure, the presence of the rotor was neglected.

From this process it emerged that **the most important parameter to consider was the height** of the structure, as its modifications proportionally influenced the current gain factor the most. The steepness of the profile and its position in the water column, which also had been considered in the study, had just a secondary effect. As increasing the height of the structure means a proportional increase in all the dimensions, it has been investigated more in detail if the obtained gain in velocity was worth the rise in construction costs.
From a preliminary analysis carried out in the study, it was shown that the rise in costs would not be justified by the increase in the current gain factor, as this kept almost constantly around a value of 2, from 1.9 to 2.2, for structure's height from 1.5 up to 25 m. Anyway it was reported that this aspect needs some further investigation.

Another result provided by the study was that **a convex shaped profile determines lower forces on the structure, improving its stability.**

This lead to consider an optimized geometry where the height was limited and the profile was convex.

(c) Power production

The simulations aimed at the power production estimate of the optimized geometry were conducted on a 3-D structure.

The power evaluation model had to be adapted to the CFD simulations, where the peculiar movement of the rotor could not be reproduced, and had to be modelled in an original way. The two limit cases of no rotational speed and maximum torque (limit case #1), and maximum rotational speed and no torque (limit case #2) could be represented by the simulations. As both of them correspond to a zero power production situation, their results were combined to achieve an estimate of the optimal power production.

As shown in the results of the physical tests, the optimal power production *PPopt* was assumed to be achieved for half of ω_{max}. This was evaluated in a setup where the rotor had no blades, representing the limit case #2 where no forces could be exterted on the rotor, from the values of velocity of the flow around it.
Assuming a linear relationship between ω and M, the torque corresponding to $\omega_{max}/2$ is $M_{max}/2$. This was obtained in the simulations considering a setup with blades, which represented the limit case #1. As in the simulations they acted as fixed walls against the flow, the pressure exterted on them, and hence the forces and the torque, were maximum.

Finally the optimum power production was evaluated as

$$\boldsymbol{PPopt = 0.25 \cdot \omega_{max} \cdot M_{max}} \quad \textbf{[W]}$$

The power production for the optimized geometry with the dimensions listed in Tab. 1.2, was estimated to be 0.2 MW and **0.44 MW** respectively under 3 and 4 m/s incoming flow.

h=	12 m	height of the structure
L=	55 m	width of base structure
l=	10 m	length of the blades
Hw=	3 m	height of the blades
ø=	7m	diameter of the rotor
p=	1 m	depth of the rotor in the base
d=	50 m	water depth

Table 1.2 – Dimensions considered in the simulations

The results showed this optimized geometry could actually lead to an improvement in the power production, taking into account the limited length of the blades considered in the study (only 25% of what used in the model test, see Tab. 3.3).
The simulations prooved to be reliable, as they were able to reproduce under the same conditions the results achieved by the tests on the 1:20 scale model with a good accuracy.

The present study

The main objectives of the present study are:

(a) Evaluate the yearly power production of a Tideng under real flow conditions typical of a possible scenario for deployment, the Faroer Islands [7].
(b) Determine the economic feasibility of Tideng, based on material costs and selling prices for the energy produced.
(c) Evaluate the convenience of using sidewalls relativeley to the economical feasibility of the device.
(d) Investigate the influence of the height of the structure on the current gain factor and on the economical feasibility

The results show an average yearly power production, evaluated over the real tidal cycle at the straight between *Streymoy* and *Sandoy*, Faroer Islands, of **8.15 GWh** (Fig. 1.4).
Under these circumstances the economical feasibility of the device is justified only by selling prices of **above 0.09 €/kWh**.

The use of sidewalls has shown to determine a small increase in the power production, enough to compensate the minor rise in costs, negligible when compared to the overall material cost. As a result the cash breakeven selling price is almost the same (0.1 € kWh), but the solution with sidewalls determines a slightly higher income when the selling prices increase (Fig. 3.3).
In a 2-D situation the increase in the height of the structure determines instead a significant raise in the current gain factor and consequently in the power production. This would allow lowering the selling prices needed to achieve the cash breakeven. This positive effect stops at heights around 15-20 m, starting then to have a negative influence. This aspect should be further investigated in a 3-D situation.
Finally, a new formulation for the evaluation of the current gain factor for a 2-D case is proposed.

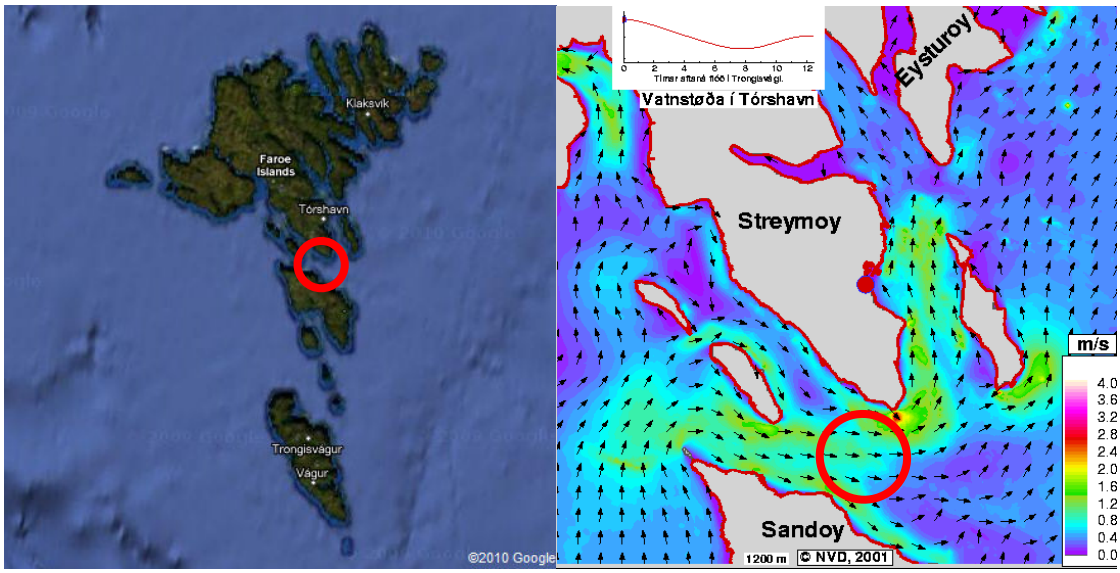

Figure 1.4 – The reference location for the tidal cycle used in the study, [7]

2. SETUP OF THE STUDY

Outline

The study is carried out by means of CFD simulations, considering both 3-D and 2-D situations.
The 3-D case has been considered to evaluate the yearly power production of a Tideng under a real tidal cycle at the chosen location. A comprehensive analysis of the power produced and material costs is carried out, leading to conclusions relatively to the economical feasibility of the device, in terms of the necessary selling price which would justify its construction. Such analysis is carried out in two different cases: with and without sidewalls.
The 2-D geometry has been used to model the effect of the height of the structure on the current gain factor and the economical feasibility of the device.

Method

The geometry considered is the standard one, with trapezoidal base and cylindrical rotor placed on the sea bottom (Fig. 2.1).

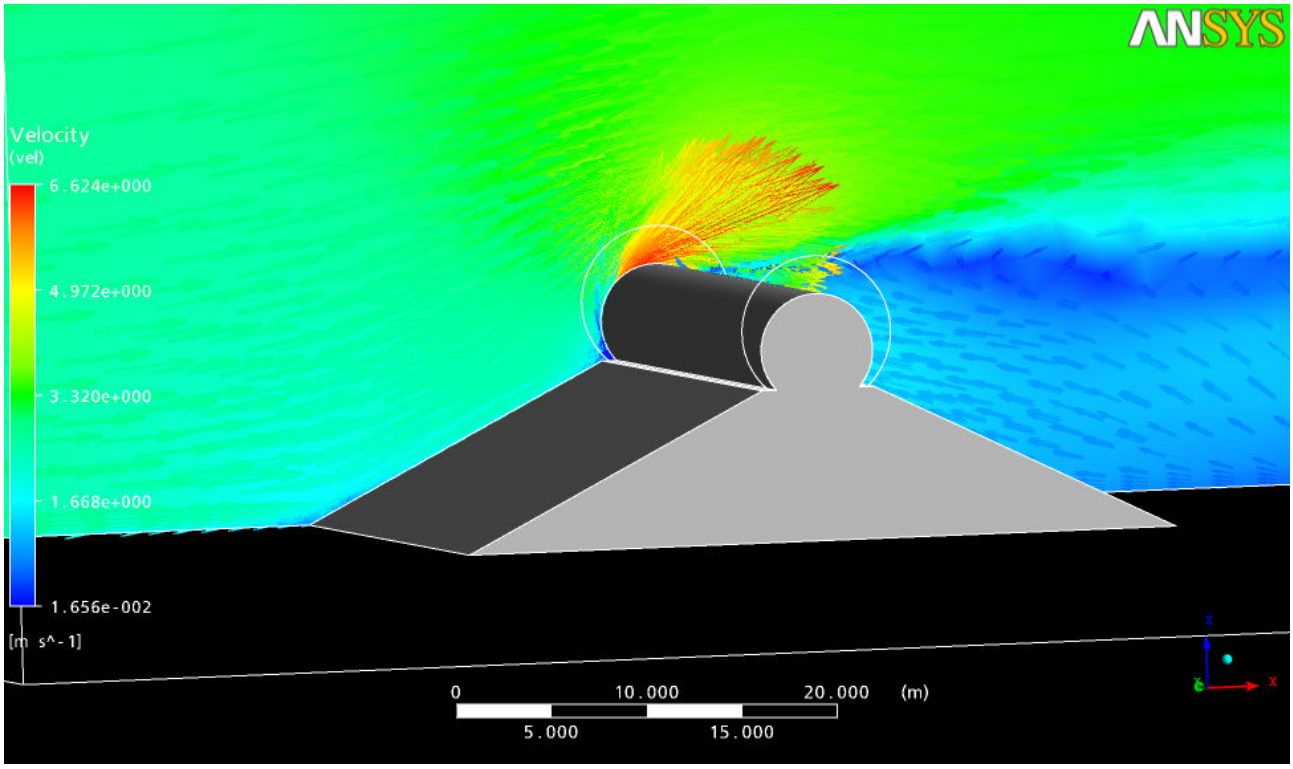

Figure 2.1 – The 3-D device considered in the simulations

Respect to the previous study carried out by means of CFD simulations [3], the power evaluation model here considers only the case without blades. During the simulations with sidewalls it emerged in fact that the flow over the rotor was so different from the one expected at a steady state, when considering the setup with blades, that such difference in flow pattern could not be neglected: the observed flow could not be considered representative of a steady state situation.
Under the focusing effect of the sidewalls indeed, the flow was completely deflected by the first blades and a significant turbulence eddy was created right on the top of the rotor, between blades #1

and #2 (blades are counted from left to right clockwise), as it can be observed in Fig. 2.2.

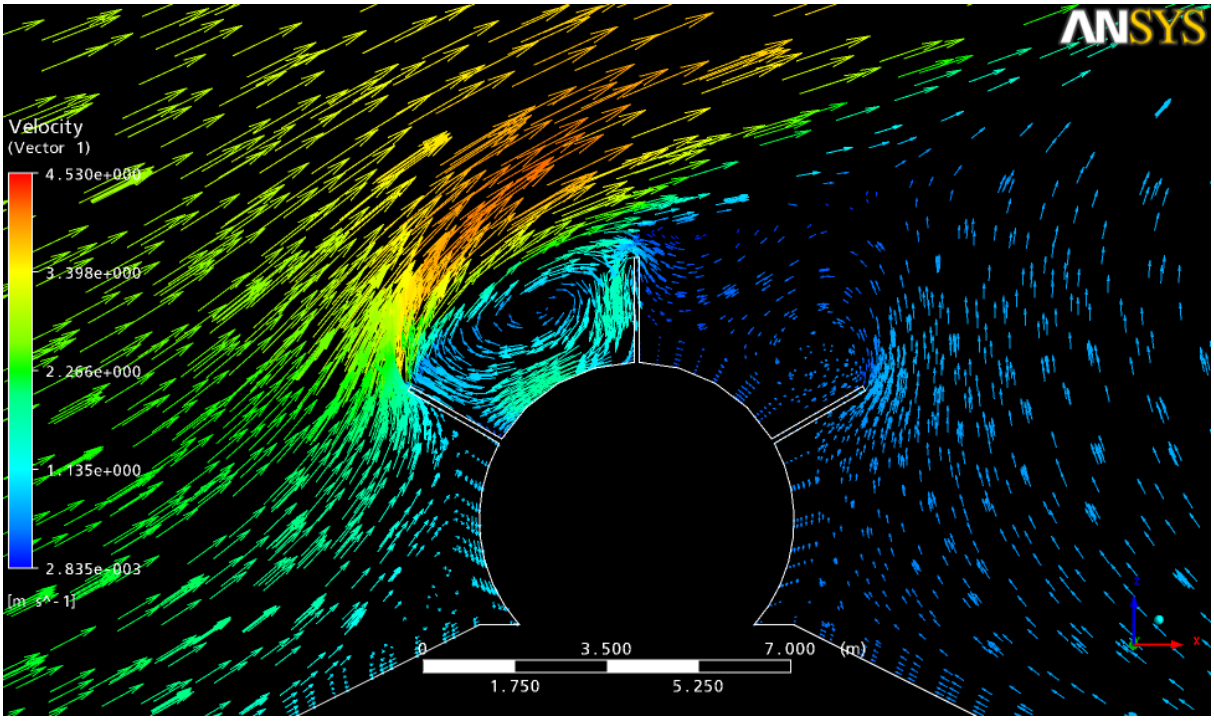

Figure 2.2 – Flow over the rotor with fixed blades, representative of a startup condition

This situation is unrealistic under a steady state condition as the rotating blades would not oppose firmly to the flow as they do in the simulations. This determined results not according to the desired physic situation, as in some case even negative x-forces on blade #2 have been observed. As a consequence the power evaluation model was changed so to consider only the setup with no blades, which well represents a real steady state situation.

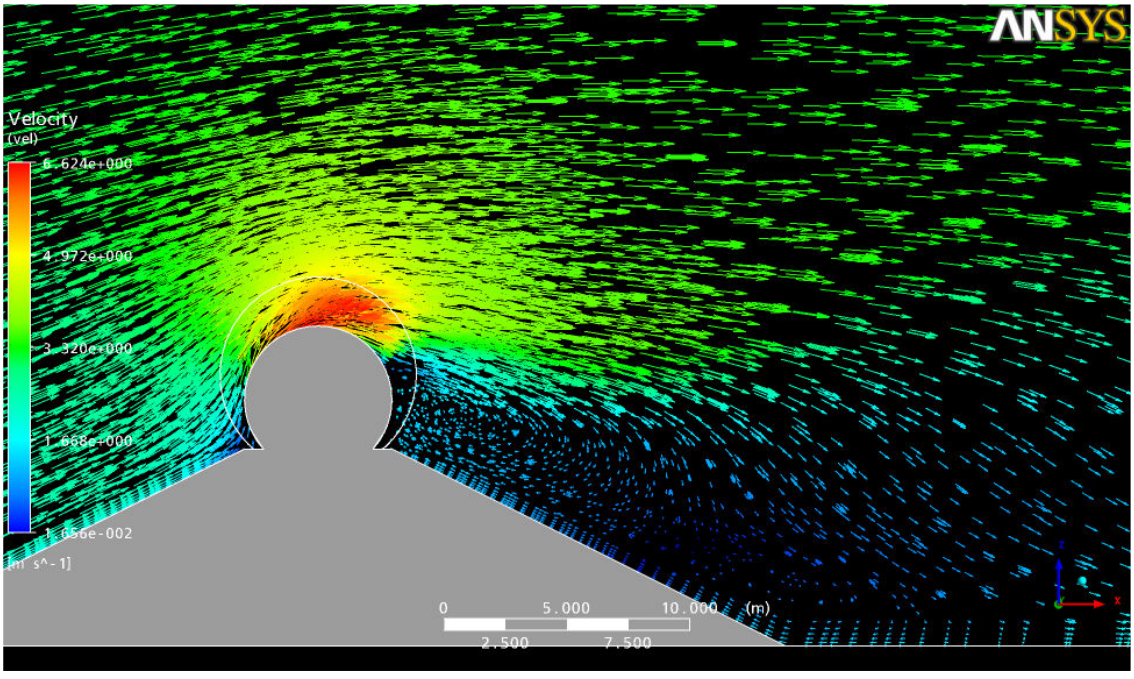

Fig 2.3 – The flow pattern in the case of no blades, representative of a steady state condition

The new formulation of the model evaluates the forces on the blades as originated by the dynamic pressure exerted by the flow on some *virtual blades*, 2-D regions of the fluid domain with the exact dimensions and location as the real blades.

Forces on the virtual blades

The forces on the blades are originated by the total pressure exterted on them by the flow. As the effect of the gravity is neglected in the simulations by considering a non-buoyant flow, the total pressure has two components: the static pressure, p_s, and the dynamic pressure, p_{dyn} (*Bernoulli's theorem*).
The first one is exerted by the fluid on a wall surface, while the second one is proportional to the square of the flow velocity.
Previously, by considering the forces acting on fixed blades, the only component of the pressure considered was the static one ($p_{tot} = p_s$), as the velocity of the flow was locally turned to zero in correspondence of the blades and its energy was totally converted into static pressure.
If we do not consider the blades we can still evaluate the total pressure exerted by the fluid on the virtual blades, which in this case is given by the dynamic pressure: $\boldsymbol{p_{tot} = p_{dyn} = \frac{1}{2} \cdot \rho \cdot Urel^2}$. *Urel* is the relative velocity of the flow respect to the virtual blade, ρ is the water density.
The force acting on each virtual blade is therefore calculated as $\boldsymbol{F_{dyn} = p_{dyn} \cdot A}$, being A the surface of the virtual blade, and the torque as $\boldsymbol{M_{dyn} = F_{dyn} \cdot b}$, where b the distance between the centre of the rotation and the point of application of the F_{dyn} at the centre of the blade.

Current gain factor

As the results of the simulations provide the field of velocity in the whole fluid domain, the current gain factor can also be determined for the different values of U_{IN} considered. The increased value of velocity *U'* is estimated as the average velocity over the volume of water close to the rotor, the same volume which is swept by the rotating blades, which is the region directly involved in the power production (see Fig. 2.4).

Rotational speed

The rotational speed is obtained under the following assumption: in a steady state situation, as we are considering, the equilibrium is reached between the flow forcing the rotation and the resistance of the rotor to move. In such a situation the velocity of the blades will be the same as the velocity of the surrounding fluid.
As the movement of the rotor is forced only by the component of the flow perpendicular to the virtual blades, we cannot use *U'* to estimate the equilibrium velocity. Indeed *U'* is an average on a volume where the direction changes consistently, so that we cannot assume any global value for it.
The approach used in the study is to consider the average of the velocity components perpendicular to each of the virtual blades, named *Ur*. This is regarded to be an acceptable approximation of the equilibrium velocity, as it assumes implicitly that the rotational speed is determined only by the component perpendicular to the blades, being at the same time an average value through all the fluid volume of interest. More details on the determination of *Ur* are in appendix A.
The maximum rotational speed is therefore calculated as the ratio between *Ur* and the average radius of the local volume considered, *R*. This represents a limit case which we are not interested in, as it corresponds to null power production due to the fact that *Urel = 0*.
From the results of the study (Fig. 3.3) it emerges that the optimal power production, *PPopt*, corresponds to a rotational speed of $\omega_{opt} = \omega_{max}/3$.

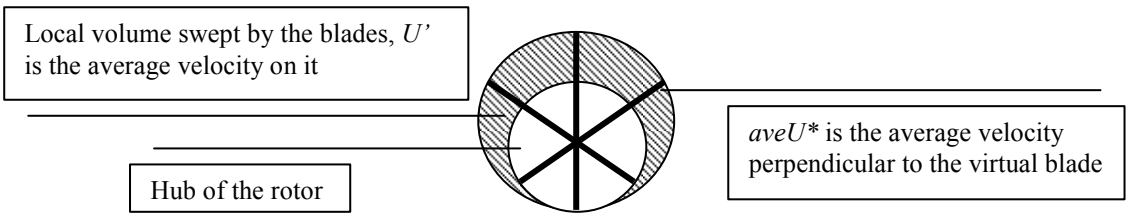

Figure 2.4 – The local volume considered around the rotor

Relative velocity

The value of *Urel* is given for each virtual blade by the difference between the component of the freestream flow perpendicular to it and the velocity corresponding to the rotational speed ω, calculated at the centre of the blade: $U(\omega) = \omega \cdot b$.
The freestream flow speed changes with the rotational speed, due to the sweeping effect of the rotating blades. At low ω the flow can still be locally characterized, and the average value of the flow perpendicular to the blade can be used as freestream velocity for each blade. At high ω instead the flow is more uniform, as previously assumed, and *Ur* has to be used for all the blades. In between this two limit situations, as is the case of optimal power production, the freestream velocity is given as a function of ω (see Tab. 2.1).

It is underlined that only the component of the flow perpendicular to the virtual blades has to be considered in the evaluation of the dynamic pressure.
A detailed description of the elaboration of the CFD results performed in order to get the component of the relative velocity perpendicular to each of the virtual blades is summarized in appendix A.

Power production

The power production *PP* is finally estimated as

$$\boldsymbol{PP = \omega \cdot M_{tot}} \quad \textbf{[W]}$$

being M_{tot} the sum of the M_{dyn} on all the virtual blades.

The global procedure followed is resumed in Tab. 2.1, and discussed more in detail in appendix A.

*AA_U** [m/s]	Average on the Area of the virtual blade of the velocity component perpendicular to it
Ur = average (*AA_U**)	Equilibrium velocity around the rotor
R [m]	Average radius of the local volume surrounding the rotor
ω [rad/s]	Rotational speed of the rotor
$\omega_{max} = Ur/R$ [rad/s]	Maximum rotational speed of the rotor
$\omega_{opt} = \omega_{max}/3$ [rad/s]	Rotational speed corresponding to the optimal power production
b [m]	Distance from the centre of rotation to the centre of the virtual blade

$U(\omega) = \omega \cdot b$ [m/s]	Velocity of the rotating virtual blade
$TSR = \omega / \omega_{max}$	Tip speed ratio
$Urel = [AA\_U^* \cdot (1\text{-}TSR) + Ur \cdot TSR] - U(\omega)$ [m/s]	Relative velocity of the flow respect to the virtual blade
$p_{dyn} = ½ \cdot \rho \cdot Urel^2$ [Pa]	Dynamic pressure exerted by the flow on each virtual blade
$F_{dyn} = p_{dyn} \cdot A$ [N]	Dynamic force acting on each virtual blade
$M_{dyn} = F_{dyn} \cdot b$ [N · m]	Dynamic torque acting on each virtual blade
$M_{tot} = \sum M_{dyn}$ [N · m]	Total dynamic torque acting on the rotor
$PP = \omega \cdot M_{tot}$ [W]	Estimated power production
$PP_{opt} = \omega_{opt} \cdot M_{tot}$ [W]	Estimated optimal power production
U'[m/s]	Average velocity of the local volume surrounding the rotor
$Cg = U'/U_{IN}$	Current gain factor

Table 2.1 – Outline of the power evaluation model

Geometry and mesh features

The device considered in the 3-D simulation is 8 m high, with a 1:2 steep and straight profile, a rotor diameter of 6 m and 3 blades 2 m high and 80 m long. The centre of rotation of the turbine is 10 m above the sea bed, and is the origin of the reference system adopted.
The base is made by 0.4 m thick concrete, while the rotor and blades are of 0.1 m thick steel.

In the cases when sidewalls have been considered, they are placed at both ends of the structure symmetrically to the longitudinal and cross planes. They are 78 m long, 30 m high and made of 0.5 m thick concrete.

The fluid domain extends 50 m before the device and 150 m after, being in total 238 m long. The width is 120 m on each side of the device, which is in total 320 m. The water depth is assumed to be constant d = 50 m.

The mesh is tethraedrical, with a generic volume spacing of 5 m and refining close to the device. It also includes prismatic elements in the boundary layer close to the bottom, the surface of the device and the sidewalls.
The maximum dimension of the surface elements on the base structure and sidewalls is 1 m, while for the rotor this is 0.5 m.
The fluid region after the rotor is refined up to 2 m in order to have more precise estimate of the turbulent flow generated by the presence of the device. The turbulence model used in the simulation is the Shear Stress Transport (SST).

Tidal cycle

The assumed tidal cycle is a semi-diurnal one, characterized by two peaks with different intesities every 24 hours. The current generated by the tide increases in magnitude when the water level is rising, becomes null at the still water (the highest water level) and then reverses its direction when the level lowers, increasing in magnitude again until the still water is reached at the lowest water level. The maximum velocity corresponds to the maximum tangent of the curve shown in Fig. 1.5.
As Tideng is characterized by a symmetrical design it works under both flow directions, so that the tidal stream cycle is the one shown in Fig. 2.5a. This continuous pattern is discretized at intervals of 1.5 h so to be described by a limited number of simulations but still being representative of the real one. The method of discretization consisted in dividing the 12 hours period in 8 intervals of 1.5 h. The value of U_{IN} calculated at the lower extreme of each of these intervals is then assumed as constant over an interval of equal length and symmetric respect to the mentioned extreme. Finally the lowest and highest remaining parts of the time domain are assumed to be $U_{IN} = 0$. In this way the number of velocities to simulate is limited to four, namely 2.5, 3.5, 2.12 and 3 m/s.
The discrete tidal cycle is shown in fig 2.5b.

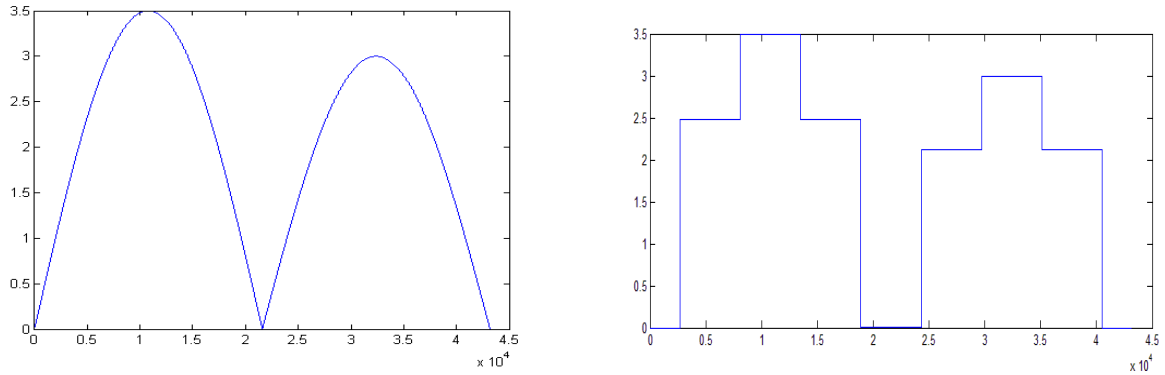

(a) (b)

Fig 2.5 – The continuous (a) and discretized (b) tidal cycle simulated, U_{IN} (m/s) over time (s)

Investigation of the height effect

Some 2-D simulations are performed on a 2 m wide domain. The geometry considered is the same descripted above, except for the heigth of the structure, which varies assuming the values of 6, 8, 10, 12, 16, 20, 24 m. The base of the structure is also varying according to h in order to keep a constant steepness of the profile of 1:2.

The refinement in correspondence of the turbulence zone, being out of the interest of the simulations, is eliminated, while the mesh is refined up to 0.2 m at the rotor surface in order to have more precise results on the current gain factor, which is estimated as $Cg = U'/U_{IN}$.

All the simulations are run under a constant flow speed of 3 m/s at the inlet.

3. RESULTS

The results shown in the following are relative to a Tideng 80 m long and 8 m high, with a straight profile of 1:2 steepness, a rotor diameter of 6 m and 3 blades 2 m high. The base structure is made of 0.4 m thick concrete, while the rotor is made of 0.1 m thick steel (see Fig. 3.1).
Results are achieved with a precision (RMS) of 0.001 m/s on the velocity and 0.0001 Pa on the pressure.

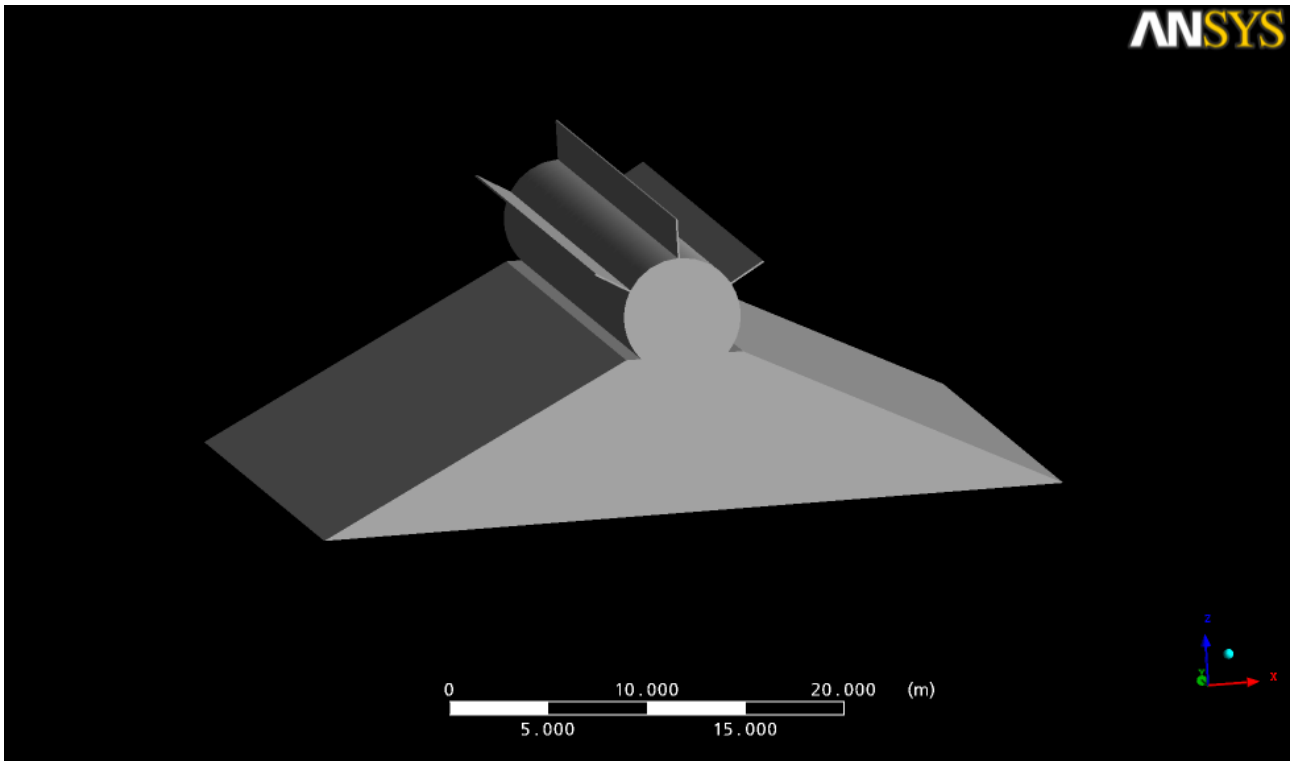

Figure 3.1 – Tideng as considered in the simulations; here the real blades are shown, which in the study have been substituted by *virtual blades* with the same dimensions and position

Power production

In Tab. 3.1 are listed the values of power produced during the considered the tidal cycle, while Tab. 3.2 summarizes the total energy output during periods of 12 h, one day and one year. All values are relative to the optimal conditions (TSR = 0.3) and both basic geometry and the case with sidewalls are considered.

Dt (hours)	Uin (m/s)	Basic geometry (MW)	With sidewalls (MW)
0 - 0.75	0	0	0
0.75 - 2.25	2.5	0.97	0.99
2.25 - 3.75	3.5	2.66	2.78
3.75 - 5.25	2.5	0.97	0.99
5.26 - 6.75	0	0	0
6.75 - 8.25	2.12	0.59	0.6
8.25 - 9.75	3	1.67	1.73
9.75 - 11.25	2.12	0.59	0.6
11.25 - 12	0	0	0

Table 3.1 – Optimal values of power produced over considered intervals

	Basic geometry	With sidewalls
PP opt (12h)	11.2 MWh	11.5 MWh
PP opt (1 day)	22.3 MWh	23.0 MWh
PP opt (1 year)	**8.15 GWh**	**8.41 GWh**

Table 3.2 – Energy output over 12 h, 1 day and 1 year

Fig. 3.2 shows the power curve of the turbine, extrapolated from the results obtained under the different flow conditions simulated in the study. The values of power produced are expressed per unit width, so that they can be compared with the result of the previous tests [1] [2] [3].

Nevertheless it has to be noted that in general all the dimensions of the device assumed in this study are different from the ones previously considered (see Tab. 3.3). They can be directly compared only respect to the model test ones, which had practically the same dimensions being the device just slightly lower (7 m in full scale instead of 8 m as in the CFD), where such difference is considered negligible.

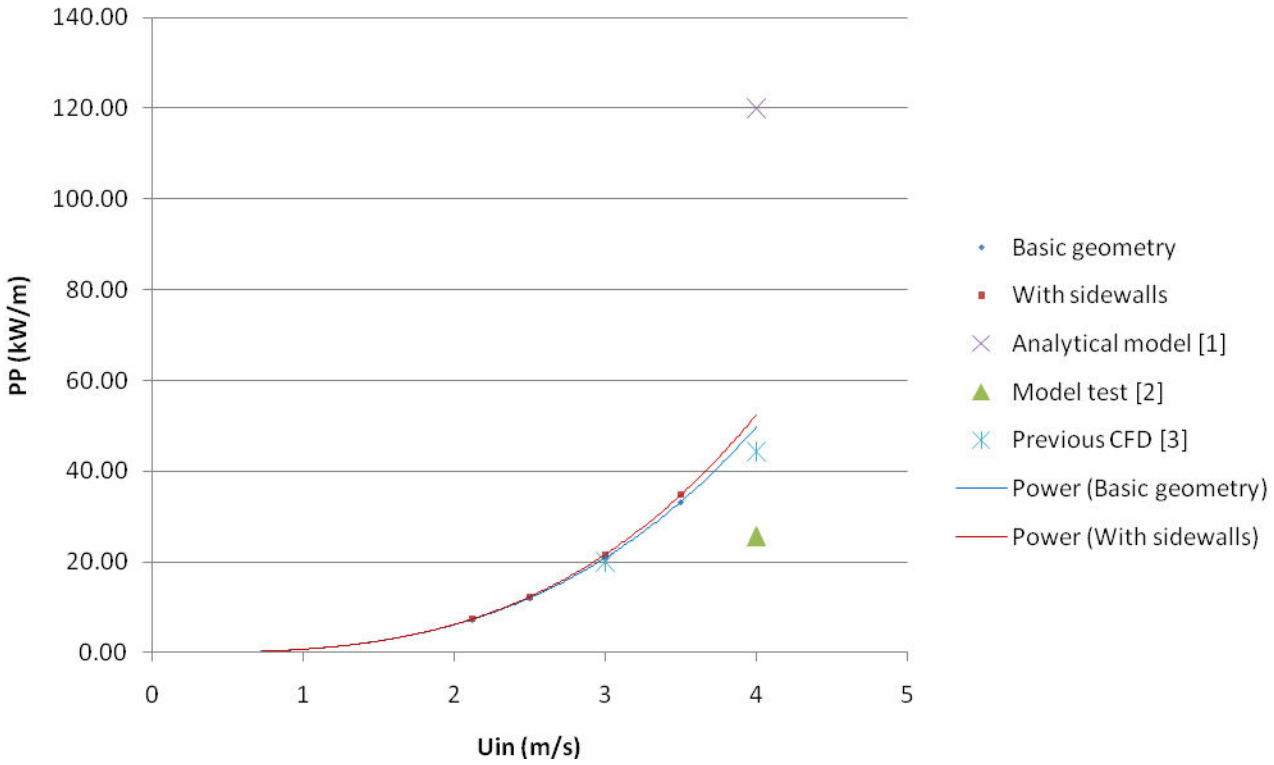

Figure 3.2 – Power curve of the turbine, extrapolated from the CFD results

To better evaluate the performances of the device under different flow conditions, the power coefficient *Cp* is used [6]. This is the ratio between the energy produced and the total kinetic energy of the flow available at the capture area *Ac* of the device, which as mentioned is the shadow area originated by the device. This is equal to the area of a vertical section passing through the centre of rotation (= $(h+(ø-1)+H_w) \cdot l$). The total kinetic energy is proportional to the cube of the undisturbed flow velocity: $Pke = ½ \cdot \rho \cdot Ac \cdot U_{IN}^3$.

Tab. 3.3 shows the power coefficient for the two cases simulated and for the previous studies. It is evident its independency from the flow conditions, as it is constant for the different values of U_{IN} considered in the CFD simulations. It is instead dependent on the relative velocity between the flow and the blades of the rotor, the tip speed ratio, as shown in Fig. 3.3.

	DHI [1]	Model test [2]	Prev. CFD [3]	Basic geometry				With sidewalls			
d (m)	30	54	50	50				50			
h (m)	12	7	12	8				8			
ø (m)	6	6	7	6				6			
Hw (m)	2	2	3	2				2			
Lw (m)	20	38	10	80				80			
Uin (m/s)	4	4	4	2.12	2.5	3	3.5	2.12	2.5	3	3.5
U' (m/s)	10	-	5.55	2.67	3.15	3.782	4.415	2.66	3.142	3.778	4.42
Cg	2.5	-	1.39	1.26	1.26	1.26	1.26	1.25	1.26	1.26	1.26
PP (MW)	2.40	0.975	0.444	0.59	0.97	1.67	2.66	0.6	0.99	1.73	2.78
PP (kW/m)	**120**	**25.7**	**44.4**	**7.34**	**12.1**	**20.9**	**33.3**	**7.44**	**12.4**	**21.6**	**34.8**
Ac (m^2)	380	532	210	1200				1200			
Ac/m (m)	19	14	21	15				15			
Pke (MW)	12.5	17.4	6.89	5.86	9.61	16.6	26.4	5.86	9.61	16.6	26.4
Pke (kW/m)	**623**	**459**	**689**	**73.2**	**120**	**208**	**330**	**73.2**	**120**	**208**	**330**
Cp	**0.19**	**0.06**	**0.06**	**0.10**	**0.10**	**0.10**	**0.10**	**0.10**	**0.10**	**0.10**	**0.11**

Tab 3.3 – Power coefficient *Cp*

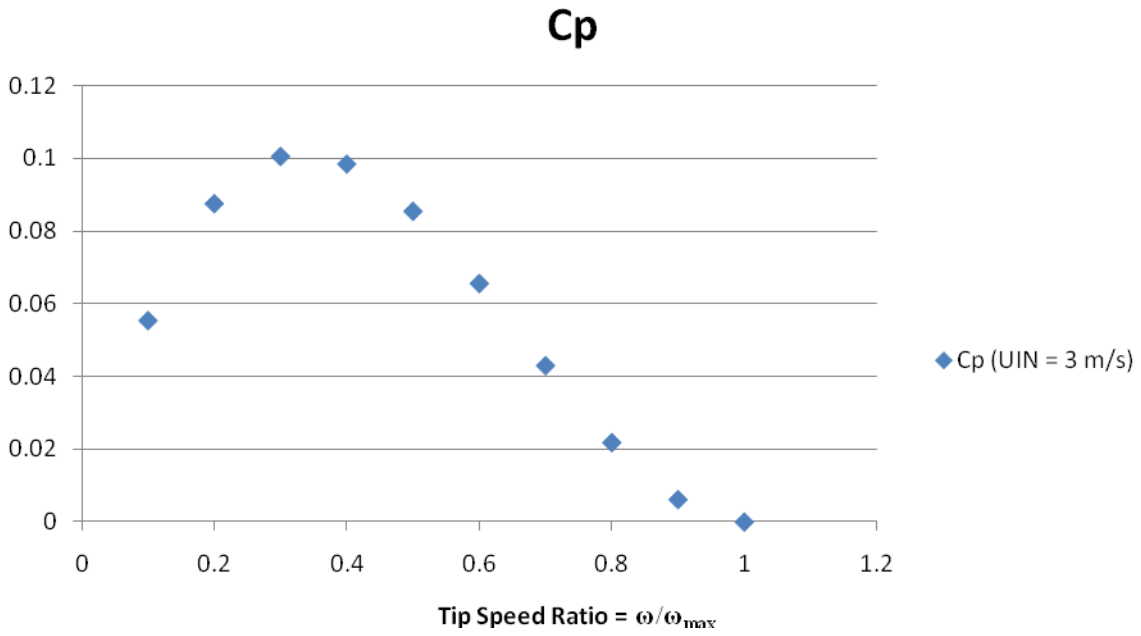

Figure 3.3 – *Cp* for different tip speed ratio

Forces on the blades

The maximum forces acting on the blades are the design values needed for the manufacturing. These are **19.5 kN/m** and 20.1 kN/m respectively for the basic geometry and the case with sidewalls, corresponding to a situation of extreme flow conditions (U_{IN} = 3.5 m/s) almost perpendicular to the blades, when these are vertical as in the case of virtual blade #2. These values are calculated from the dynamic pressure originated by the average flow speed on the virtual blade's section, and are therefore average values over the whole 80 m length of the device.

The design torque is originated by the maximum force relatively to the point of contact between the blade and the hub of the rotor. As the lever arm in this case is 1 m, the corresponding torque per meter width is **19.5 kNm/m** for the basic geometry, 20.1 kNm/m in the case with sidewalls.

Economic feasibility

Tab. 3.4 summarizes dimensions and costs of the different components of device. An economic analysis is showed in Tab. 3.5 based on the selling price (€/kWh) needed in order to achieve the cash breakeven within the estimated lifetime of the device, 20 years. Fig. 3.4 shows possible profits for different selling prices.

dimensions						
Base Height (m)	Base Width (m)	Length (m)	Rotor Diameter (m)	Blade Height (m)	Sidewalls Height (m)	Sidewalls Width (m)
8	38	80	6	2	30	78

	Thickness (m)	Volume (m3)	Material	Specific Weight (kg/m3)	Weight (kg)	Price (€/kg)	Material cost (M€)
Base	0.4	2'447.10	concrete	2400	5'873'050	0.19	1.12
Rotor	0.1	348.45	25% steel1	7900	2'752'765	6.25	10.5
			75% steel2			3	
Sidewalls	0.5	2'340.00	concrete	2400	5'616'000	0.19	1.07

	Basic Geometry	**With Sidewalls**
Rated power (MW)	2.66	2.78
Generator price (M€/MW)	1.00	1.00
Generator cost (M€)	2.66	2.78
Device total cost (M€)	**14.3**	**15.5**

Table 3.4 – Dimensions and costs of the device

	Basic Geometry	**With sidewalls**
Yearly production (GWh/year)	8.15	8.41
Lifetime (years)	20	
Total production over lifetime (GWh)	163	168
Total cost (M€)	14.27	15.46
Cash breakeven selling price (€/kWh)	0.09	0.1
Income (M€)	14.66	16.82
Profit (M€)	0.39	1.36

Table 3.5 – Economic feasibility analysis

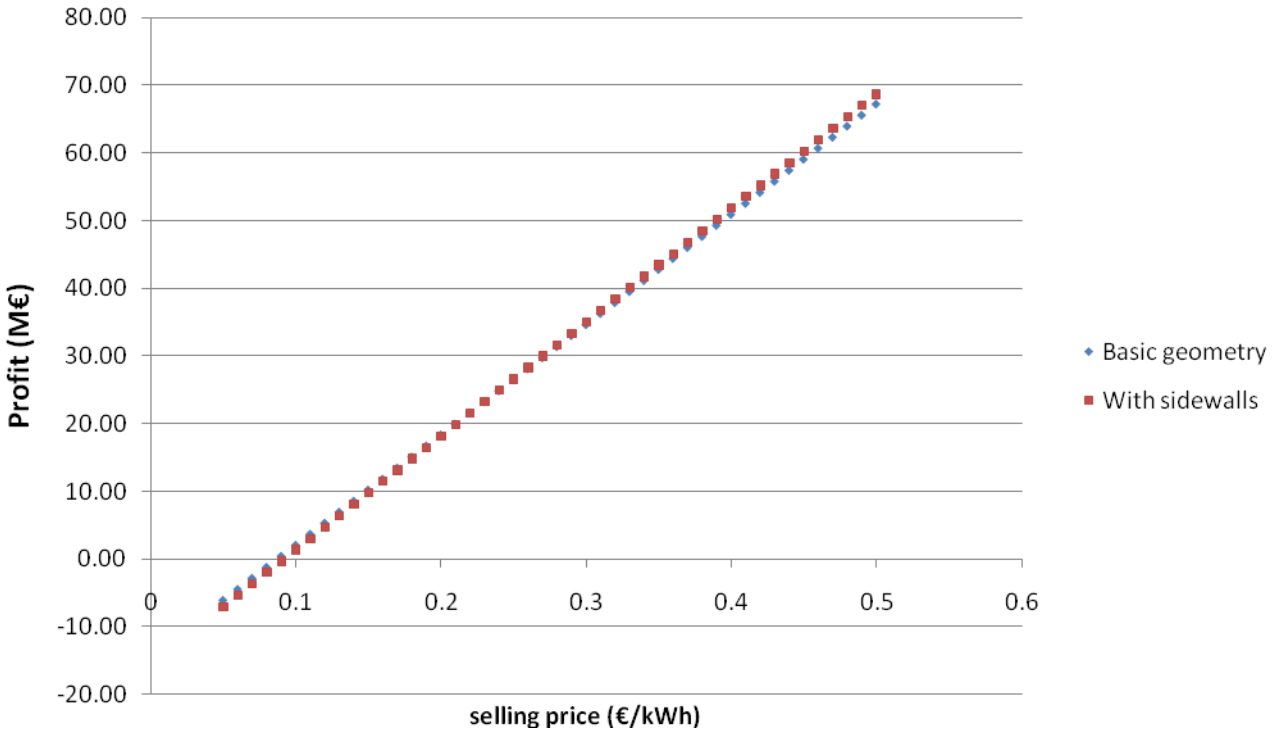

Figure 3.4 – Profit for different selling prices

Fig. 3.5 shows the selling prices needed to achieve the cash breakeven during the lifetime of the device for different values of *h*. As they are based on the results of the 2-D simulations, to not create confusion about the actual prices needed in a real 3-D configuration, these are normalized relatively to the optimal selling price, found for *h*=16 m.

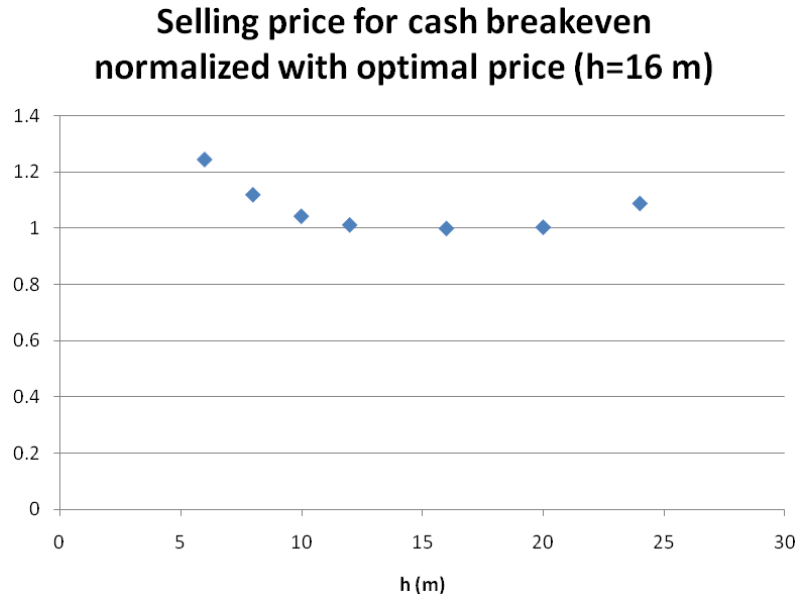

Figure 3.5 – Selling price required for different *h* in a 2D case; values are normalized relatively to the lowest one, found at *h*=16 m

Current gain factor

The 2-D analysis is used to determine an expression for the current gain factor. In Fig. 3.6 the prediction made by the formulation proposed by the analytical model [1] is compared with the results of the CFD simulations. A new formulation for the evaluation of *Cg* in a 2-D case is proposed in Fig. 3.7.

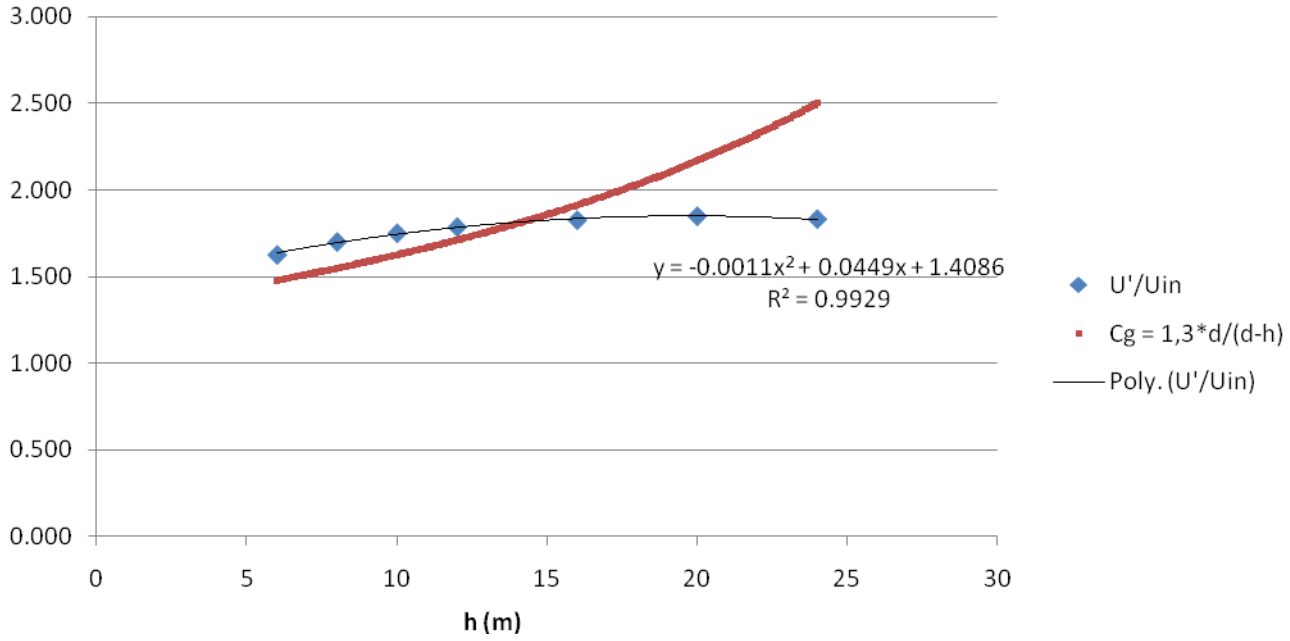

Figure 3.6 – Comparison of the *Cg* predicted by the analytical model [1] with the one obtained from the results of the 2-D simulations

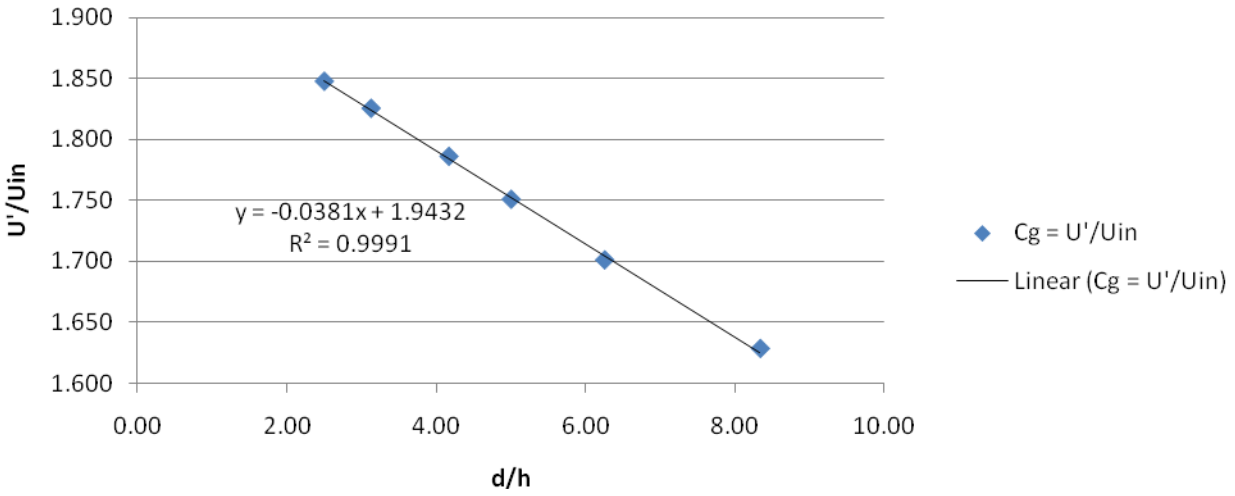

Figure 3.7 – Proposal for a new *Cg* formulation based on CFD results, valid in a 2-D case

4. DISCUSSION

Novelty

Tideng is a new tidal stream energy converter. According to our knowledge no similar device/idea has been presented internationally until now. The rotor is the innovative and novel aspect of the device. A paddle streamer is the closest existing technology to be compared with the invention.

Power production

Under the simulated flow conditions, a Tideng 8 m high and 80 m long, with a rotor of 6 m diameter and blades 2 m high can produce **8.15 GWh/year**, 8.41 GWh/year in the case sidewalls are used (Tab. 3.2). The accuracy of the calculated power production is estimated to be within plus/minus 25%.

The possibility of using a higher number of blades, 4 instead of 3, has also been considered in the study. Nevertheless the results showed that the increase in the yearly power production, 14.7% and 23.7% respectively for a basic geometry and with sidewalls, was retained to be too low when compared to the increased complexity in manufacturing the rotor and to the rise in material costs.

The efficiency of the device, measured by the power coefficent (Tab. 3.3), is higher than shown in the model test and the previous CFD calculations. *Cp* is indeed found to be in all the cases considered in the simulations around a value of 0.1, which means that the turbine is actually able to extract around the 10% of the available kinetic energy of the flow. The turbine can be compared with the turbine from a paddle streamer, which will typically have an efficiency in the order of 5-10%, while a traditional ship propeller typically will have an efficiency in the order of 30%; this difference can be explained by the fact that in Tideng the active blades do not take advantage of the lift effect.

The *Cp* obtained by the analytical model [1] is almost the double respect to the one estimated by the CFD simulations. This is probably due to the overestimate of the *Cg* carried out in the analytical study, which cannot be justified in terms of geometrical differences (see Tab. 3.3), resulting in too optimistic performances of the device.

It is worth noting that the power production model used in the present study considers the optimal power production at a tip speed ratio of 0.3, as done in [1], while experimental data [2] states that the optimal power production is achieved for a rotational speed which is the half of the maximum. This is in contrast with what is shown in Fig. 3.3, where the optimal power coefficient, and therefore the best performances of the turbine, is actually achieved for a $\boldsymbol{\omega = 0.3 \cdot \omega_{max}}$ under the assumptions of the power evaluation model used.

Economic feasibility

The accuracy of the cost related calculations is estimated to be within plus/minus 50%. The study considers material costs and general costs for the generator, neglecting other important components such as operational and maintainance costs and grid connection costs which can be a significative part of the total cost for the deployment of the device. Also, it has to be considered that the costs of a first prototype will be higher than the cost per unit when mass production would be achieved, due to scale economy considerations.

In the basic case considered, selling prices should be **above the 0.09 €/kWh** (Tab. 3.5) in order to have a positive profit within the estimated lifetime of the device. This price is still high compared to fossil fuels (coal, natural gas and oil), for which energy costs are in between 0.04 and 0.06 €/kWh [4], and also compared to some renewables energy sources like wind, geothermal, hydropower and biomass, which can keep the selling prices below 0.1 €/kWh [5]. Still, this figure is favourable with the current cost for the ocean energy, which is estimated to be in between 0.2 and 0.5 €/kWh, and below solar photovoltaic and thermal (respectively 0.25 to 0.50 €/kWh and between 0.12 and 0.34 €/kWh) [5].

Considering the lower bond of the current figures on selling prices for ocean energy (0.2 €/kWh), under the condition considered in the study the net income expected within the lifetime of the device is above 18 M€.

The use of sidewalls improves the power production of the device. The reason for this is that the sidewalls partly limit the losses due to the cross flows generated as a boundary effect at end of the device. These cannot be exploited by the rotor as their velocity component perpendicular to the blades is small or null. Such cross flows are locally limited by the use of sidewalls or in regions far from the end when considering very long devices. In both these situations the longitudinal component of the flow is enforced, until the limit case where the boundary effect becomes negligible and the flow is completely bi-dimensional, leading to a much higher current gain factor and therefore lower selling prices as demonstrated by the 2-D simulations carried out in the study. Nevertheless such limit situation can be economically unsustainable, so that some loss due to the cross flows has to be accepted.

In the configuration considered in the study the effect of the sidewalls, even though present, is very limited. It determines an increase in the power production which is just sufficient to balance the raise in cost due to the construction of the sidewalls, as demonstrated by the fact that the cash breakeven selling price is almost the same (0.1 €/kWh). Fig. 3.4 shows that the actual benefit deriving from the use of sidewalls appears evident only for selling prices above 0.22 €/kWh; in this condition the total profit achieved during the device's lifetime is bigger.

Further research is required to evaluate the influence on the power output of the shape of the sidewalls and of their position relatively to the end of the device.

From the 2-D simulations it emerges that also an **increase in height of the structure favours the power production, as it influences positively the current gain factor** (Fig. 3.6). This improvement is so effective that it compensates the raise in material cost, making it possible to lower the selling prices (Fig. 3.5). Such positive influence becomes progressively less evident and

disappears around values of h = 15÷20 m, where the trend is inverted. We can therefore consider 15 m as the upper limit for h. This aspect should also be further investigated on a 3-D setup, where probably it will be less evident due to effect of the mentioned cross flows.

Current gain factor

The 2-D simulations show that the formulation considered in the analytic model [1] for the evaluation of the current gain factor does not follow the results of the CFD (Fig. 3.6). As mentioned, this is probably the reason of the much higher value of *Cp* found for the case considered. In particular, at constant d, it overestimates the current gain factor starting from values of h around 15 m, where the positive effect of the increase in height stops. As previously said, *Cg* becomes constant around a vaue of h = 15÷20 m so that it is desirable to limit h to these values as no further improvement is achieved for larger structures.

A new **model for the evaluation of *Cg* in a 2-D situation** is proposed (Fig. 3.7), based on the very good linear dependency observed between the non-dimensional parameter d/h and the current gain factor obtained by the simulations. This is characterized by an extremely high correlation (R = 0.999) up to values of $h = 0.4 \cdot d$, which on the basis of what has been said about the need of limiting the height of the structure seems reasonably the whole field of application of Tideng.

It is worth noting that the power production estimate achieved in the 2-D case is around 3.3 times higher than in the 3-D case considering the same conditions of h = 8 m and U_{IN} = 3 m/s. This is due to the energy dispersed by the cross flows and by the flow passing on the side of the device in the 3-D case, while in a 2-D case the current is entirely passing over the rotor, perpendicularily to it. *Therefore the figures relative to the 2-D case should not be extrapolated to a 3-D case* just by multiplying the power production for the desired width, as this would lead to neglect the mentioned effect and to consistently overestimate the power production. For the same reason economical calculations for the 2-D case has been omitted.

5. SUGGESTED FURTHER RESEARCH

The next steps in the development of the device should be carried out in order to accomplish the following main objectives:

- The rotor and its blade moving system should be analyzed by a mechanical engineer in order to realistically assess its feasibility and cost and to determine eventual drawbacks;
- A more accurate and comprehensive economic analysis should be carried out by a specialist in the sector, as this is the part entailing the highest uncertainties in the present study. This is to be intended as a first rough estimate of the costs, based mainly on the material's costs. It is thought that the accuracy on the figures relative to costs and selling prices can be improved by a more precise analysis;
- Tests or simulations should be carried out on the model considering a rotor actually rotating. This is highly desirable as the assumptions needed by the present model still limit the accuracy of the power production figures given.
- Optimization of the shape and position of the sidewalls is required, as well as further investigation of the effect of h on the current gain factor in a 3-D case.

6. References

[1] Utilization of energy in tides and flowing water in rivers – M. B. Bryndum and R. Deigaard, DHI - Institute for Water and Environment, 2004;

[2] Model test of Hilleke Power System water turbine – Kurt Hansen, Sintef Fisheries and Aquaculture, 2007;

[3] Geometry optimization of Tideng tidal stream power converter by means oof CFD simulations and power production estimate – Stefano Parmeggiani, Aalborg University – Department of Civil Engineering, 2009;

[4] EIA – Green econometrics research, 2007;

[5] World energy assessment 2004 – UNDP;

[6] Assessment for performance of Tidal Energy Conversion Systems – European Marine Energy Centre, 2008;

Web references:

[7] http://www.sleipnir.fo/setur/nvd/havfrodi/Sjovarfall/index_en.htm

Appendix A

In order to estimate the power production using only the setup with no blades some assumptions have to be made.

Although this situation well represents a steady state flow on a Tideng under normal operating conditions, some of the key variables involved – such as the relative velocity, the forces on the blades and the rotational speed – have to be derived from the results of the simulation as they are not a direct output of the CFD. During this process the physics of the phenomenon has to be taken carefully into account, so that the representation of the system is as close as possible to the real situation.

Here the main assumptions of the model are resumed and discussed, toghether with the procedure through which the mentioned variables are obtained from the CFD results.

The rotational speed

The main assumption behind the determination of the rotational speed is that *at a steady state the equilibrium is reached between the active and resisting forces involved in the rotation of the turbine*, being the former determined by the pressure exterted by the flow, and the latter by the resistance offered by the turbine to rotate into a viscous fluid as the water.

Under this condition the rotational speed will be the maximum, ω_{max}, and the blades will move with the same velocity as the surrounding fluid. The determination of the rotational speed passes therefore through the estimate of such equilibrium velocity.

As said above the rotation is forced by the pressure exerted on the blades by the fluid, which in the case considered is the dynamic pressure on the virtual blades. Only the component of the flow perpendicular to the blades should be considered in the evaluation of the pressure, as this is defined as the normal force applied on the area of the blades. Hence the directionality of the flow should be taken into account in the evaluation of the equilibrium velocity.

The average velocity over the local volume surrounding the rotor, *U'*, cannot be considered for the purpose as we have no information about its direction, since it is an average value over a region where the direction of the flow changes consistently.

From the results of the CFD we can instead derive the component of the flow's speed perpendicular to the virtual blades. For each blade the orientation in the three dimensions is known, and the CFD can calculate the average value of the velocity component in the x, y and z direction on the blade's surface. Therefore, by knowing the relative angle, it is possible to obtain the resulting value of the flow's velocity perpendicular to each virtual blade *AA_U**. The * sign denotes the component perpendicular to the virtual blade, while the prefix AA denotes that the value is an Average over an Area.

To consider an average value over the whole volume surrounding the rotor, the average of the *AA_U** relative to the 3 virtual blades is calculated. This value, named *Ur*, is considered as the equilibrium velocity and $\omega_{max} = Ur/R$, being *R* the average ratio of the local volume considered respect to the centre of rotation. The main advantage of considering *Ur* instead of *U'* is that we ensure that the rotational speed is actually due only to the forcing component of the flow.

Moreover the average of the average values on the 3 virtual blades represents quite well the average value through the whole fluid domain surrounding the rotor, called the *local volume*. It was observed that if we divide this volume into 4 parts delimited by the virtual blades, the average velocity on each of these parts can be well represented by the average velocity on one of the virtual blades: the first and last parts are well represented by virtual blade #3, the second part by #2 and the third part by #1 (see Fig. A.1). Therefore the average between the average velocities on the virtual blades well represents the average on the local volume, and the accuracy can be increased by considering twice virtual blade #3.

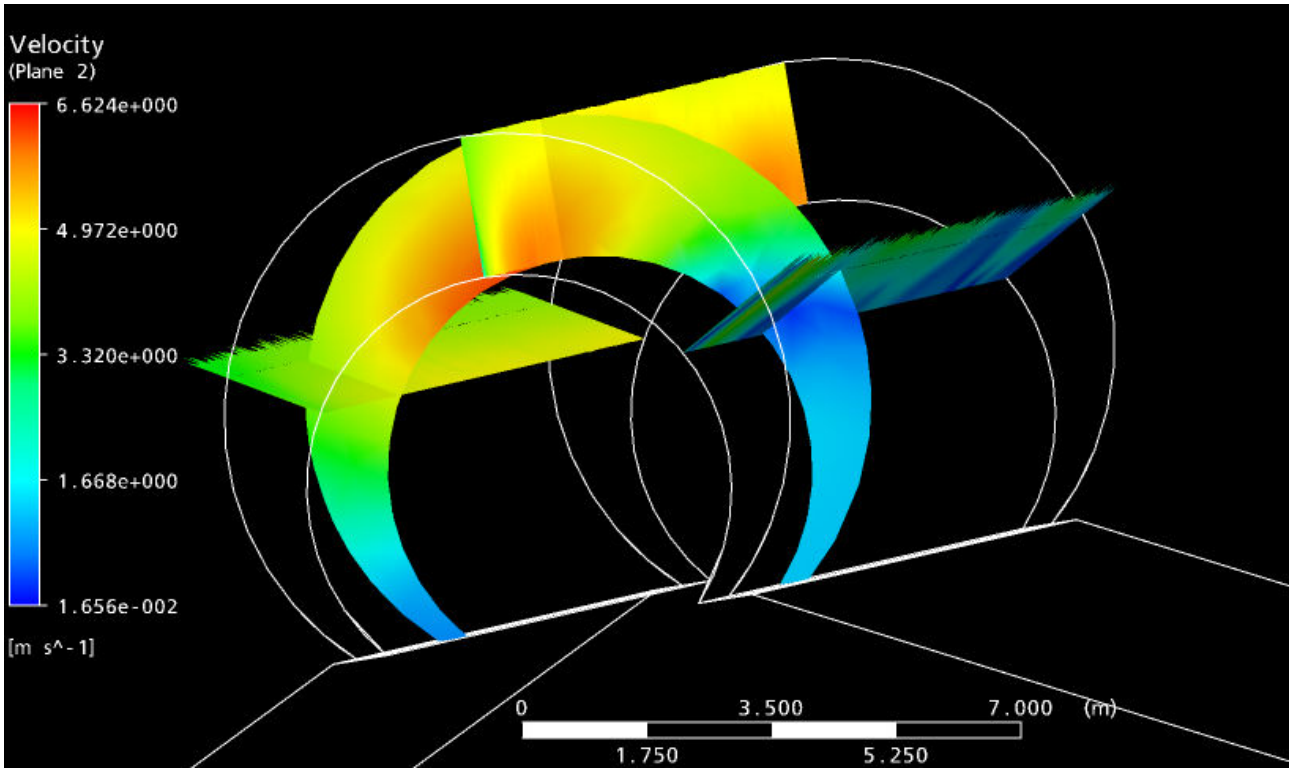

Figure A.1 – Velocity on the virtual blades and the local volume

The rotational speed ω is varied considering different tip speed ratios $TSR = \omega / \omega_{max}$.

In the evaluation of the optimal power production a $TSR = 0.3$ has been considered, being therefore $\omega_{opt} = 0.3 \cdot \omega_{max}$.

The relative velocity to consider

The power evaluation model used in the study considers the dynamic force exerted by the fluid on the blades. This is proportional to the square of the velocity of the flow relative to the blades: *Urel*.

The value of *Urel* is the difference of the freestream velocity near to the virtual blades and the velocity of displacement of the blades due to the rotation $U(\omega) = \omega \cdot R$.

The freestream velocity is also influenced by the rotational speed, as for low ω the local flow field at each virtual blade still has to be considered, while for high ω the assumption made about the equilibrium velocity leads to consider a more uniform flow field. In the first case the freestream velocity is different for each virtual blade, and corresponds to the average velocity on it (*AA_U**), while in the latter case *Ur* has to be assumed as relative velocity for all the virtual blades.

In an intermediate condition between maximum and minimum ω, as it is the case of optimal power production, *Urel* is therefore a function of ω:

$$Urel = [AA\_U^* \cdot (1 - TSR) + Ur \cdot TSR] - U(\omega) \qquad \text{(A1)}$$

where the tip speed ratio is used to describe the effect of the different ω in uniforming the flow around the rotor.

The effect of the choice of the freestream velocity is shown in Fig. A.2, where the power coefficient for different *TSR* is drawn for

- Freestream velocity = *AA_U**, this is correct for a situation when the tip speed ratio is low and the blades move relatively slow compared to the surrounding flow. This means that the local differences in the flow are still important.
- Freestream velocity = *Ur*, according to the main assumption of the model this is correct for high tip speed ratio.
- Freestream velocity = mixed value (A1), valid for all *TSR*.

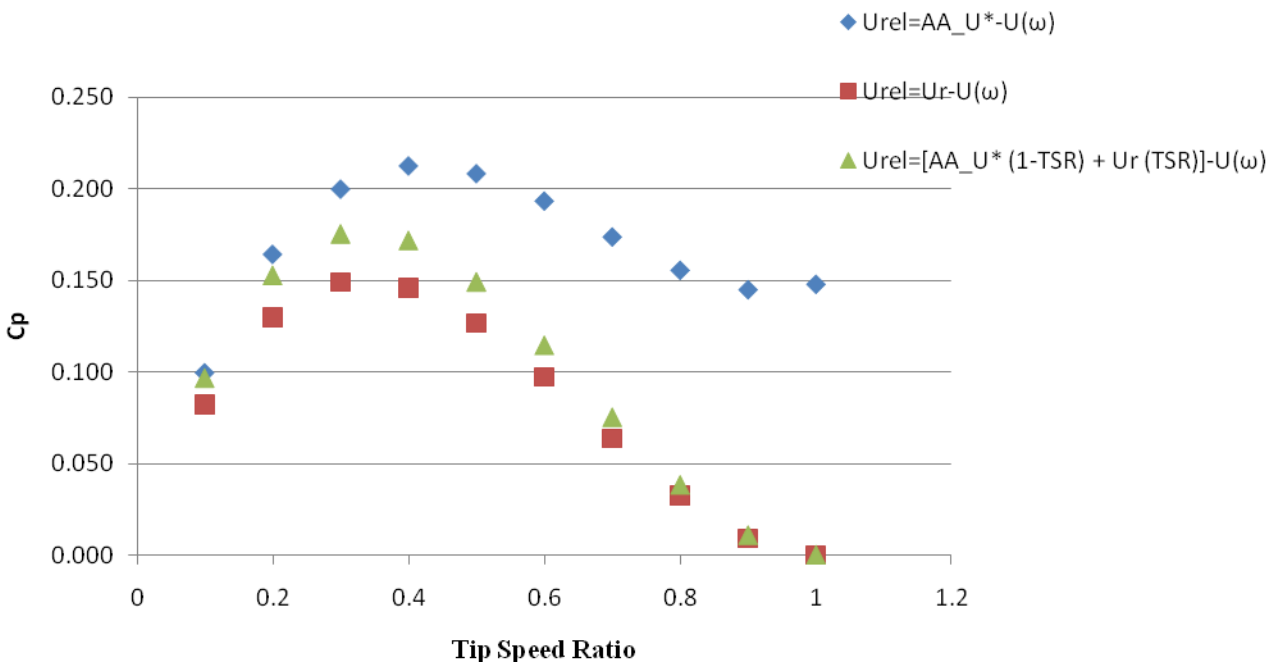

Figure A.2 – Effect of the freestream velocity chosen in the evaluation of *Urel*

It has to be underlined that the case where only the local effect are considered (blue dots) is not a good choice, as it gives wrong estimates for high *TSR*, such as positive power production for $\omega = \omega_{max}$ where we know that $PP = 0$ as $Urel = 0$. On the other hand by neglecting such effect at all (red dots) the power production is underestimated, especially for the lowest *TSR*.

The use of a mixed formulation where the solution is biased towards one limit case or another depending on the *TSR* assumed is therefore considered to be a good choice.

For the optimal power production the local effect are considered slightly more than the sweeping effect due to the rotation.

Evaluation of the forces on the virtual blades

Two important aspects should be considered in the evaluation of the forces on the virtual blades strarting from the flow velocity:

1. The dynamic pressure is determined by the component of the flow perpendicular to the blade.

2. The flow determines a positive force on the blades, but there is also a negative pressure on the backside of the blades exerted by the resistance to move of the fluid volume in between them.

1. Considering the perpendicular component of the flow

The pressure forces are for definition perpendicular to the considered surface. Therefore, evaluating such pressure forces from the velocity field, only the component of the velocity perpendicular to the surface (in our case the virtual blades) has to be considered.

The procedure followed for each virtual blade to estimate such component consisted in register the average values of the x and z component of the flow velocity. The y component is always parallel to blades and does not determine any pressure on them. These values, named *AA_Ux* and *AA_Uz*, are a direct output of the CFD software used.

As the orientation of the blades in the three dimensions is known and the direction of the two velocity recorded is respectively x and z, the relative angle is also known and the components perpendicular to the blade can be calculated: *AA_Ux** and *AA_Uz**. The resulting normal component is therefore $AA\_U^* = AA\_Ux^* + AA\_Uz^*$.

Regarding the velocity of the blade due to the rotational speed $U(\omega)$, as this is estimated from ω it is always perpendicular to the blade.

2. Negative pressure on the backside of the virtual blades

The fluid volume in between the blades is drag by them during the rotation. As these have to exert a certain force to move such volume, it exterts a counter force on the blades, opposing to the rotation and finally decreasing the power production. Such negative force is due to the acceleration of the fluid and to its inertia to move.

The first component is $F = m \cdot a$, where m is the mass of the fluid volume and a its acceleration. a is null except for a startup situation, which is not of our interest as we want to consider a steady state situation. This leads us to neglect this component.

The inertia of the fluid volume depends on its weight, but as we are considering a non-buoyant flow the effect of the gravity acceleration g on the fluid should be neglected, and therefore also the second component of the backside pressure on the virtual blades should be neglected.